Journal of Thermal Biology 123 (2024) 103939

Contents lists available at ScienceDirect

Journal of Thermal Biology

journal homepage: www.elsevier.com/locate/jtherbio

Experimental evidence of a Neotropical pest insect moderately tolerant to complete freezing

Trinidad León-Quinto [a,b], Noelia Antón-Ruiz [a,b], Roque Madrigal [c], Arturo Serna [d,*]

[a] Área de Zoología, Depto. Agroquímica y Medio Ambiente, Universidad Miguel Hernández, E3202-Elche, Alicante, Spain
[b] Instituto de Bioingeniería, Universidad Miguel Hernández, E3202-Elche, Alicante, Spain
[c] Departamento de Ciencia de Materiales, Óptica y Tecnología Electrónica, Universidad Miguel Hernández, E3202-Elche, Alicante, Spain
[d] Departamento de Física Aplicada, Universidad Miguel Hernández, E3202-Elche, Alicante, Spain

ARTICLE INFO

Keywords:
Paysandisia archon
Palm pest
Tropical insect
Lepidoptera
Cold tolerance
Water loss

ABSTRACT

Due to climate change, many regions are experiencing progressively milder winters. Consequently, pest insects from warm regions, particularly those with some tolerance to low temperatures, could expand their geographic range into these traditionally colder regions. The palm borer moth (*Paysandisia archon*) is a Neotropical insect that in recent decades has reached Europe and Asia as one of the worst pests of palm trees. Little is known about its ability to tolerate moderately cold winters and, therefore, to colonize new areas. In this work, we characterized the cold tolerance of *Paysandisia archon* by measuring its thermal limits: median lethal-temperature, LT_{50}, chill-coma onset temperature, CT_{min}, supercooling point, SCP, freezing time and freezing survival. We found that this species was able to survive short periods of complete freezing, with survival rates of 87% after a 30-min freezing exposure, and 33% for a 1 h-exposure. It is then a moderately freeze-tolerant species, in contrast to all other lepidopterans native to warm areas, which are freeze-intolerant. Additionally, we investigated whether this insect improved its cold tolerance after either short or long pre-exposure to sub-lethal low temperatures. To that end, we studied potential changes in the main thermo-tolerance parameters and, using X-ray Computed Tomography, also in the morphological components of pretreated animals. We found that short pre-exposures did not imply significant changes in the SCP and CT_{min} values. In contrast, larvae with long pretreatments improved their survival to both freezing and low temperatures, and required longer times for complete freezing than the other groups. These long-term pre-exposed larvae also presented several morphological changes, including a reduction in water content that probably explained, at least in part, their longer freezing time and higher freezing survival. Our results represent the first cold tolerance characterization of this pest insect, which could be relevant to better design strategies to combat it.

1. Introduction

The average temperature of many regions, as well as the frequency of unseasonal cold or warm periods, are progressively increasing due to climate change (Bathiany et al., 2018; Johnson et al., 2018). As this occurs, some insect species could expand their geographic range into areas that were previously too cold for their survival (de la Vega et al., 2015). This is particularly relevant in the case of pest insects, mainly those with some tolerance to moderately low temperatures and transient cold events.

Insect cold tolerance is usually characterized by different parameters, primarily the chill-coma onset temperature, survival rates at low temperatures, and the supercooling point (see Sinclair et al., 2015 for a review). The chill-coma onset temperature (CT_{min}) is the temperature at which an insect enters a reversible comatose state characterized by the cessation of voluntary movement and muscle function, rendering the insect temporarily immobile. It then provides the lowest temperature limit at which an insect can remain active and responsive to its environment (Andersen et al., 2017) and, therefore, it is crucial to determine the ability of a species to expand its geographical distribution. In the same way, the ability to survive cold exposure is quantified by the temperature range of cold injury. This interval spans from the lethal temperature LT_{100}, with 100% mortality, to the temperature above which there are no longer individuals killed by cold. Within this interval,

* Corresponding author.
E-mail addresses: trini.leon@umh.es (T. León-Quinto), noelia.antonr@umh.es (N. Antón-Ruiz), roque.madrigal@umh.es (R. Madrigal), arturo.serna@umh.es (A. Serna).

https://doi.org/10.1016/j.jtherbio.2024.103939
Received 5 June 2024; Received in revised form 8 July 2024; Accepted 18 July 2024
Available online 6 August 2024

a parameter widely used to characterize the ability to survive the cold is the median lethal temperature (LT_{50}), which corresponds to 50% mortality. Finally, the supercooling point (SCP) is the temperature at which the insect body fluids begin to freeze. According to the SCP and LT_{50} values, and in the absence of external ice inoculation (see Rozsypal and Košťál 2018 for insect cooled in contact with external ice), the cold tolerance strategy of insects is often classified into two broad categories: freeze-tolerant ($LT_{50} \leq$ SCP) and freeze-intolerant ($LT_{50} >$ SCP) species. Within the latter, some authors (Sinclair et al., 2015) also distinguish between freeze-avoidant and chill-susceptible species, depending on whether or not they are able to survive in a (non-frozen) supercooled state.

Insects have developed a diversity of behavioral, morphological and biochemical responses for coping with the detrimental effects of low temperature and thus survive in cold environments (Lencioni 2004; Mutamiswa et al., 2023). Each species adopts a different combination of these responses (Denlinger and Lee 2010) and requires specific study. The time scale for deploying these responses may require days or weeks of pre-exposure to moderately low temperatures, in a process often termed cold acclimation (CA). However, some insect species can deploy such responses within minutes or hours, in a process usually termed rapid cold hardening (RCH). Insect cold tolerance has been extensively studied for species native to cold areas (e.g., Koštál et al., 2016; Toxopeus and Sinclair 2018; Cubillos et al., 2018), but it is still poorly known for species inhabiting warm geographical regions. In general, tropical species have inefficient mechanisms for cold resistance and are therefore vulnerable to both seasonal and short-term low-temperature episodes. However, some of these species exhibit remarkable cold tolerance (e.g., Mutamiswa et al., 2018a, 2018b), which provides them with some resistance to events of sudden drops in environmental temperature and thermal anomalies associated with climate change. An example is the tropical insect *Gromphadorhina coquereliana,* which is able to survive partial freezing (Chowanski et al., 2015, 2017; Lubawy et al., 2019). In the same way, one of the worst palm pests in warm areas, the red palm weevil *Rhynchophorus ferrugineus*, can maintain its developmental rate at 5 °C (León-Quinto et al., 2020, 2022) and survive temperatures close to 0 °C (Martin and Cabello 2005, 2006).

Another tropical insect showing some cold-induced responses is the palm borer moth, *Paysandisia archon,* a Lepidopteran species native to South America. It was introduced into Europe and Asia in the 1990s through the international trade of palm trees (Sarto i Monteys and Aguilar, 2005; Muñoz-Adalia and Colinas 2020), and it is currently considered one of the most damaging palm pest insects in the invaded non-native areas. Little is known about the tolerance of this species to low temperatures and, therefore, about its real ability to deal with moderately cold winters and colonize new areas considered nonviable so far. Recent studies (León-Quinto et al., 2024) have observed a phenotypic response of *Paysandisia archon* after long-term exposure to low temperatures. This response includes biochemical changes, such as the accumulation of potentially cryoprotective substances in the hemolymph, as well as several morphological changes, including a reduction in hemolymph volume and, therefore, partial dehydration.

The primary objective of the present study was to characterize for the first time the cold tolerance of *Paysandisia archon* by measuring its thermal limits (CTmin, SCP, LT_{50}, freezing time and freezing survival). Another key objective of our study was to investigate whether this species has the ability to improve its cold tolerance after either short or long pre-exposure to sublethal low temperatures. Within this latter objective, we were also interested in analyzing whether the morphological changes previously reported (León-Quinto et al., 2024) for this species after a prolonged period of pre-exposure to cold had some cryoprotective role and whether such morphological changes also appeared after a short period of pre-exposure to low temperatures. To measure the morphological response to cold stress we used X-ray Computed Tomography, a modern technique that provides precise measurements of the volume percentage of the different tissues and internal components of an insect, including the digestive tract and fluids such as hemolymph. Knowledge of the low-temperature performance of this species is relevant to better understand the factors that determine its geographical distribution and, therefore, to design more effective management strategies for the control of this pest insect.

2. Materials and methods

2.1. Insect sampling

Wild larvae were collected from September to March in two collection campaigns: 2022–2023 and 2023–2024. All larvae were removed from infested palm trees (*Phoenix dactylifera*) located in the palm grove of Elche, Spain, a UNESCO World Heritage Site. After collection, the larvae were immediately taken to the laboratory, where we selected those in healthy conditions and with active mobility. Larval masses ranged from 1.5 g to 8.8 g, thus covering all developmental stages (up to the ninth instar) except for the earliest three.

To analyze the thermotolerance of this species, as well as the possible effect of different pre-exposures to moderately low temperatures, the selected larvae were distributed into four pretreatment groups with similar ranges of masses and collection dates.

a) C0: Control animals in basal conditions, without any treatment before thermotolerance tests.
b) P2h: Larvae pre-exposed for 2 h at a temperature of 1.0 ± 0.5 °C. The purpose of this group was to analyze whether a short pre-exposure to moderately low temperatures led to any significant change (rapid cold hardening) in the subsequent tolerance of this species to severe cold conditions.
c) P7d: Larvae pre-exposed for 7 days at a temperature of 1.0 ± 0.5 °C. We used this group to analyze whether a long pre-exposure to moderately low temperatures led to any significant change (cold acclimation) in posterior thermotolerance tests.
d) C7: Since the larvae of the P7d-group stopped feeding, we also considered another control group formed by larvae that remained without feeding for 7 days at a controlled temperature of 23 ± 1 °C. Thus, temperature was the main environmental difference between the P7d and C7 groups.

2.2. Survival rates and median lethal temperature

All temperature measurements for the present study were taken using a Type-K thermocouple connected to a data logger (TC08, Pico Technology, United Kingdom), which recorded temperature every 1s. In a first series of experiments, conducted in 2022–2023, animals were placed individually in a temperature-adjustable chamber (Alpicool, USA), where they remained for 2 h at a constant (±0.5 °C) temperature. We considered seven temperature values ranging from −12 °C to 0 °C and used 10 larvae for each temperature setting. After treatment, the larvae were returned to 23 °C and their survival was monitored for 14 days. The final (at day 14) survival rates $s(T)$ at different temperatures were fitted to a logistic regression model, $s(T) = 100/[1 + e^{-(\alpha+\beta T)}]$, α and β being the fitting parameters, so that $LT_{50} = -\alpha/\beta$ was the median lethal temperature (50% survival).

2.3. Chill-coma onset temperature, supercooling point, freezing time and freezing survival

Each larva was individually placed in a 50 ml Falcon tube, with the thermocouple tip fixed inside, and then placed in the temperature-adjustable chamber. The behavior of the larva throughout this process was visualized by a video camera. After equilibration for 10 min at 20 °C, the temperature was decreased 0.5 °C every 5 min, implying an effective cooling rate of 0.1 °C/min, similar to that used in most previous studies (e.g., Kleynhans et al., 2014; Roeder and Daniels 2022). At the

end of each temperature step, we tested whether the animal managed to stand up again after rotating the tube. When it no longer reacted in a coordinated way, we recorded the temperature as CT_{min}.

Once the larva entered into chill-coma (then, with reduced mobility facilitating its manipulation), it was introduced up to the end of another 15 ml Falcon tube. The tip of the thermocouple was placed at the final narrowing of the tube, so that it remained in close contact with the larva. To better immobilize the animal, we also inserted a piece of cotton that lightly pressed on it. The tube was then placed in the temperature-adjustable chamber with a cooling rate now fixed to 0.5 °C/min (Zheng et al., 2017). The supercooling point (SCP) and the time required for complete freezing were then quantified from the individual cooling curve of each larva. To visualize this procedure, Fig. 1 shows a representative freezing curve for *Paysandisia archon*, where the red solid line represents the temperature at the insect body surface, T_s, while the blue dashed line is the temperature of the surrounding air, T_a. As in other systems (see, e.g., Figure 1.1 of Pham 2014, and Fig. 2 of Kang et al., 2020), we observed three differentiated stages in this curve.

1) *Pre-freezing stage.* The air temperature decreases at a cooling rate b and, consequently, the insect body temperature also decreases (although remaining $T_s > T_a$ for $b \neq 0$, see Huey et al., 1992). Even when the melting point is reached, the insect remains unfrozen and continues to cool (supercooling) until nucleation begins. At this point, which we recorded as SCP, the phase change begins and the insect body temperature suddenly rises due to the large amount of latent heat released by freezing.
2) *Freezing stage.* This stage begins with the sudden increase in temperature from SCP until nearly reaching the melting point value, T_m. Once started, the freezing process is progressive. A layer of ice first forms on the surface and then gradually thickens (schematized at the top of Fig. 1). The interface between this frozen layer and the inner unfrozen region is called the *freezing front* and its temperature is T_f. This freezing front gradually moves deeper into the insect, while the outer frozen layer continues to cool (see, e.g., chapter 1 of Pham 2014). As a consequence, the temperature T_s on the insect surface gradually decreases, $T_s < T_f$, although slowly due to the latent heat conducted from the freezing front to the body surface. The freezing stage is then observed in Fig. 1 as an almost horizontal line, with a small decreasing slope (a horizontal line would correspond to a homogeneous freezing throughout the interior of the insect). The end of the phase change (complete freezing) was identified in the cooling curve as the instant at which a slope change occurred (the intersection of red dotted lines in Fig. 1). The time elapsed from the detection of SCP to the freezing completion then corresponded to the individual freezing time, t_F. Its value depends on multiple factors (Pham 2014; ASHRAE 2006) and is given by the balance between the latent heat flux released at the freezing front, the heat flux transported by conduction through the frozen layer and the heat flux transferred by convection to the surrounding air.
3) *Sub-Freezing stage.* Once the freezing front reaches the center, the phase change is completed. The insect is essentially solid and its body temperature then decreases more sharply than during freezing, following a process similar to that of the pre-freezing stage, where no latent heat is released.

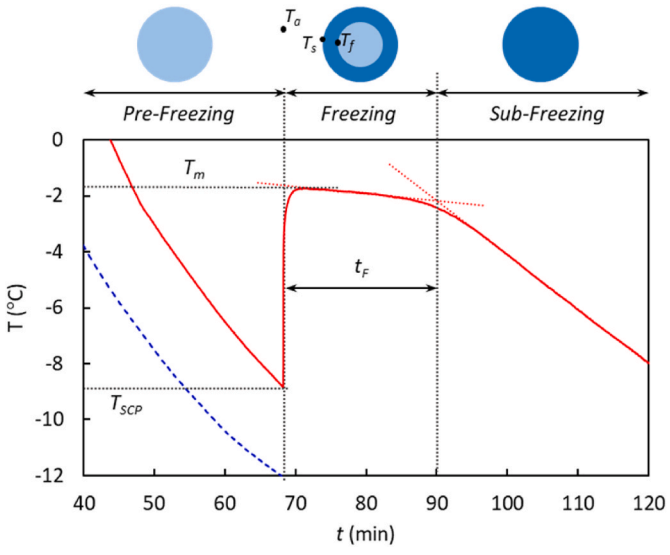

Fig. 1. Representative freezing curve for *Paysandisia archon*, showing three stages: pre-freezing, freezing, and sub-freezing. The red solid line is the temperature at the insect surface, T_s, while the blue dashed line represents the temperature of the surrounding air, T_a. The blue circles outline the insect freezing process from the outer frozen layer (dark blue) to the inner unfrozen region (light blue). (For interpretation of the references to colour in this figure legend, the reader is referred to the Web version of this article.)

To analyze freezing survival, we left each larva in the temperature-adjustable chamber for a time after SCP detection of either 3 min (partial freezing), 30 min (complete or almost complete freezing), 1 h, or 2 h (complete freezing and subsequent subcooling). The larvae were then returned to a room with controlled temperature (23 °C) and provided with food. We later observed the animals for 14 days to check their survival.

2.4. X-ray computer tomography

To study the cold-induced morphological changes experienced by this species after different pretreatments, we scanned 50 larvae with X-ray CT, a non-invasive imaging technique based on X-ray absorption. Scanning was carried out with the Albira Si system (Bruker Corporation, Karlsruhe, Germany) using its high-resolution setting (45 keV and 0.4 mA), which provides for each animal 1000 slices of 70 × 70 mm^2 and an effective spatial resolution of 85 μm (Sánchez et al., 2013). This technique generates a 3D map of the entire animal, the interior of which is divided into small volume units called voxels, as many as the system resolution allows. The 3D map contains detailed information on the tomographic density (ρ) of each voxel, so that the main morphological components (hemolymph, fat body, high-density tissues, and inner air) can be identified and quantified according to the procedure described by León-Quinto et al. (2020, 2024).

Briefly, the total volume of low-density tissues (mainly hemolymph and fat body) was quantified by counting the number of interior voxels with $-200 < \rho < 90$ HU, where HU denotes Hounsfield units. These components appear in Fig. 2a as blue-green areas. In the same way, the total volume of high-density tissues (mainly the head capsule, part of the integument, and the digestive tract) was determined from the number of voxels with $\rho \geq 90$ HU. These components appear in Fig. 2a as yellow-red areas. Within low-density tissues, hemolymph and fat body are spatially mixed. However, their respective contributions to the total volume were separated as shown in Fig. 2b: in the histogram of tomographic densities, hemolymph corresponded to a peak in the range −32 to 0 HU, so that its relative volume was quantified from the voxel numbers that exceeded the fat body background distribution (fitted to a cubic spline). On the other hand, the different high-density tissues are spatially separated, so it was also possible to separately quantify the volume of the digestive tract and that of the remaining high-density tissues. To achieve this, we analyzed all transverse slices of each specimen in an automated manner and plotted radial density profiles along lines with different angles α (Fig. 2c and d show two representative examples). After identifying in each density profile the radial distance r_{min} at which a relative minimum was observed, voxels with $\rho \geq 90$ HU and positions $r < r_{min}$ then corresponded to the digestive tract, while those with $\rho \geq 90$ HU and $r \geq r_{min}$ constituted the rest of the high-density tissues. The remaining voxels corresponded to low-density tissues

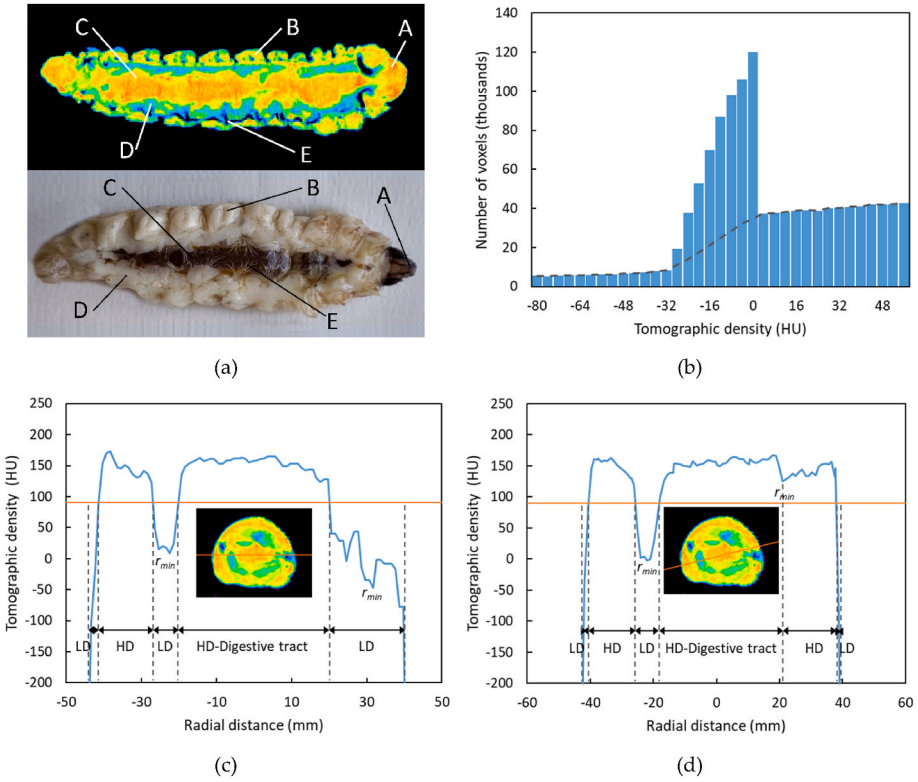

Fig. 2. Quantification from X-ray CT of the different components of each larva: a) Representative CT image of *Paysandisia archon,* where high-density (HD) tissues (A: cephalic capsule, B: integument, C: digestive tube) are the regions with $\rho \geq 90$ HU (yellow-red), while low-density (LD) components (D: fat body and hemolymph, E: tracheal air) are the regions with $\rho < 90$ HU (green-blue); b) hemolymph peak, the volume of which corresponds to the voxels that exceed the background distribution of the fat body; c)-d) two examples of radial profiles (blue curves) on the line indicated on the superimposed cross-sectional X-ray CT image. Within high-density tissues (above the horizontal brown line at $\rho = 90$ HU), the digestive tract corresponds to voxels with $r < r_{min}$, while other external tissues correspond to voxels with $r \geq r_{min}$ (r_{min} is the radial distance at which a relative minimum is observed). (For interpretation of the references to colour in this figure legend, the reader is referred to the Web version of this article.)

($-200 < \rho < 90$ HU) or internal air ($\rho \leq -200$ HU). All high-density voxels in the anal segment were added to the digestive tract, while those in the cephalic capsule were included in the remaining high-density tissues.

2.5. Statistical analysis

For each dependent variable (CTmin, SCP, t_F, etc.), we used a multifactor ANOVA-ANCOVA (MANOVA for the inner morphological components) to analyze the possible effect of different factors: collection date and larval mass (taken as quantitative factors), as well as the pretreatment group (taken as qualitative factor with nominal labels: "C0", "C7", "P2h" and "P7d"). When this latter factor was relevant, we performed post-hoc Tukey tests for pairwise comparisons between pretreatment groups. A similar procedure was used for the analysis of dependencies on survival rates, but now with temperature (in cold-stress survival) or exposure time (in freezing survival) as an additional factor. Now, the effect of the different cold pretreatments on the survival rate after freezing or severe cold stress was analyzed using Kaplan-Meier curves (Caesar 2003; Zheng et al., 2017) and different post-hoc tests: log-rang, Wilcoxon and Tarone-Ware. All statistical analyses considered a $P < 0.05$ significance level and were performed with the XLStat software package (Addinsoft, New York, USA).

3. Results

3.1. Median lethal temperature

We found that survival rates significantly depended on temperature, larval mass, and pretreatment group, while collection date did not show a significant effect (see Table 1). For C0 larvae (basal conditions), the survival rate for different mass ranges (below and above the overall average mass: 5 g) is represented in Fig. 3a as a function of temperature (light-blue curves and squares). As shown in this figure and Table 1, the LT_{50} values ranged from −8.0 °C ($m \geq 5$ g larvae) to −7.2 °C ($m < 5$ g larvae), with an overall average of −7.6 °C.

Regarding the possible dependence of LT_{50} on the pretreatment group, we found that the survival rate at $T = -8$ °C (value close to the average LT_{50} of non-pretreated C0 larvae) was higher (75%) in the P7d group than in the other groups (40, 42, 50%), see Table 2. Such a difference was statistically significant ($P < 0.05$) according to Wilcoxon and Tarone-Ware tests, but the log-rank test led to P values slightly higher than 0.05. Such a discrepancy between tests indicated that treatments mainly differed in the times of occurrence of deaths after freezing. As shown in Fig. 3b, the majority of deaths occurred during the freezing process itself in the C0, C7 and P2h groups, while in the P7d group mortality decreased and occurred a few days after freezing. Summarizing, our results indicated (although with some reservations)

Table 1
Survival rates and LT_{50}: ANCOVA and Logistic Regression.

ANCOVA			Logistic Regression and LT_{50}			
Factor	*F*	*P*	Mass	α	β	LT_{50} (°C)
Temperature	35.382	**< 0.001**	<5 g	6.714	0.938	−7.2
Date	2.710	0.103	≥5 g	5.994	0.753	−8.0
Mass	4.487	**0.037**	Any	5.972	0.784	−7.6
Group	3.089	**0.031**				

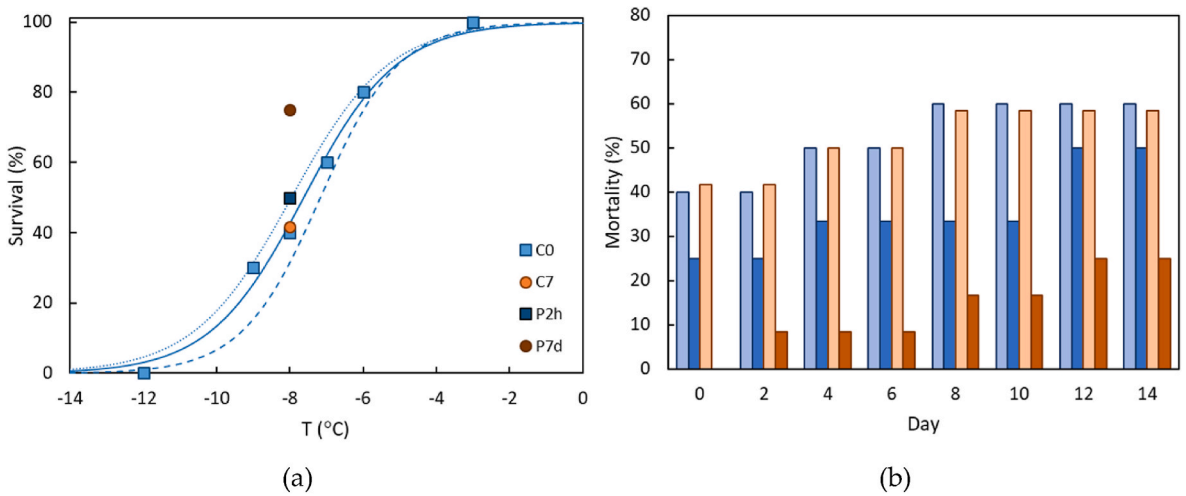

Fig. 3. a) Survival rate at day 14 for C0-larvae as a function of temperature (light-blue squares, $n = 10$ per temperature). Data were fitted to logistic regression models for all C0 larvae (solid curve), larvae with mass <5 g (dashed curve) and larvae with mass ≥5 g (dotted curve). For $T = -8$ °C, the figure also shows the survival rate for C7 (light brown circle, $n = 12$), P2h (dark blue square, $n = 12$), and P7d (dark brown circle, $n = 12$) groups, b) Cumulative mortality for 14 days after a 2 h-exposure to −8 °C for C0 (light blue), C7 (light brown), P2h (dark blue), and P7d (dark brown) groups. (For interpretation of the references to colour in this figure legend, the reader is referred to the Web version of this article.)

Table 2
Survival rates at $T = -8$ °C and Post-hoc pairwise comparisons (Kaplan Meier analysis).

Grouping					*P* values			
Group	Survival	*L*	*W*	*T*	Pair	P_L	P_W	P_T
C0	40%	(a)	(a)	(a)	P7d vs C7	0.062	**0.033**	**0.044**
P2h	50%	(a)	(a, b)	(a, b)	P7d vs C0	0.061	**0.037**	**0.047**
C7	42%	(a)	(a)	(a)	P7d vs P2h	0.214	0.183	0.198
P7d	75%	(a)	(b)	(b)	P2h vs C0	0.526	0.457	0.485
					P2h vs C7	0.575	0.476	0.518
					C0 vs C7	0.960	1.000	0.982

Note: Different letters (*a, b*) denote groups with significant difference according to *L* = log-rank, *W*=Wilcoxon and *T* = Tarone-Ware tests.

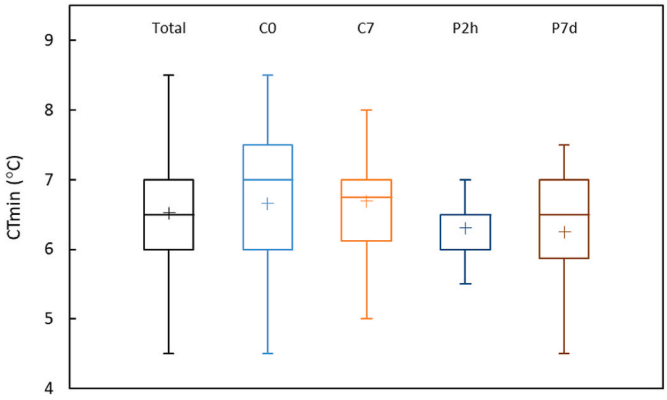

Fig. 4. CT_{min} average values (crosses) and box plots for C0 (light blue), C7 (light brown), P2h (dark blue) and P7d (dark brown) pre-treatments, as well as for all the groups together (black). (For interpretation of the references to colour in this figure legend, the reader is referred to the Web version of this article.)

that the P7d pretreatment improved the cold tolerance of *Paysandisia archon*, while the P2h pretreatment did not lead to any significant change compared to the control larvae.

3.2. Chill-coma onset temperature

We found that the average values (±S.E.) of CT_{min} were: 6.7 ± 0.9 °C for C0 ($n = 49$), 6.7 ± 0.8 °C for C7 ($n = 18$), 6.3 ± 0.8 °C for P2h ($n = 18$) and 6.3 ± 0.9 °C for P7d ($n = 20$), see Fig. 4. No significant differences were found among groups ($F = 1.428$, $P = 0.239$), with an overall average value of 6.5 ± 0.9 °C for all the pre-treatment groups ($n = 105$). We also found no significant dependence on collection date ($F = 2.969$, $P = 0.088$) or larval mass ($F = 1.936$, $P = 0.167$). Therefore, the ability of this species to remain active at low temperatures did not improve after a prior short or long exposure to low temperatures.

3.3. Supercooling point, freezing time, and freezing survival

The average value of SCP found for *Paysandisia archon* was close to −6.5 °C (see Fig. 5), without a significant dependence on pretreatment ($F = 0.046$, $P = 0.987$), larval mass ($F = 0.363$, $P = 0.548$) or collection date ($F = 0.227$, $P = 0.635$). Therefore, this species did not exhibit a greater supercooling capacity after either short or long pre-exposure to cold. Note that such SCP values corresponded to the temperature at the larval body surface, only slightly higher than the decreasing temperature of the surrounding air. Therefore, the average SCP value was close to LT_{50} (−7.6 °C), suggesting that this species might have some tolerance to freezing.

The freezing time (from SCP detection to complete freezing) for the different pre-treatments is represented in Fig. 6 as a function of mass. We found that the freezing time significantly increased with larval mass, as well as with the duration of cold pretreatment (see Fig. 6 and Table 3). Larvae with long pretreatments (P7d group) had significantly longer freezing times than the two control groups. In larvae with short pretreatments (P2h group), a certain trend towards longer freezing times was also observed, but such an increase was not yet statistically significant.

SCP measurements were also used to analyze the freezing survival of *Paysandisia archon*. All other lepidopterans from warm areas die before or immediately after reaching their individual SCP. We found however the unexpected result that many of the *Paysandisia archon* larvae survived after being partial or completely frozen. These survival rates significantly depended on exposure time ($F = 11.656$, $P < 0.001$), larval

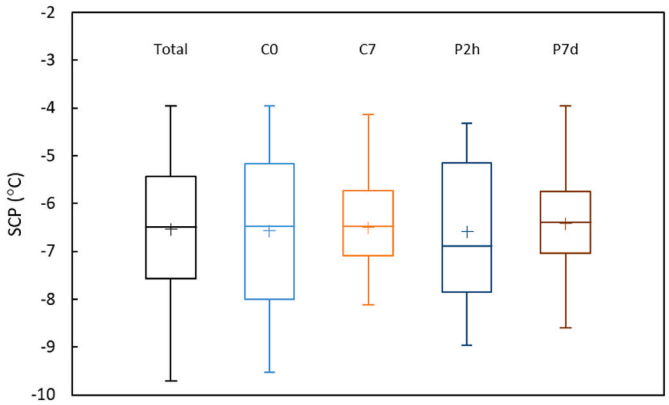

Fig. 5. SCP average values (crosses) and box plots for C0 (light blue, $n = 49$, -6.6 ± 1.6 °C), C7 (light brown, $n = 18$, -6.5 ± 1.4 °C), P2h (dark blue, $n = 18$, -6.6 ± 1.5 °C) and P7d (dark brown, $n = 20$, -6.4 ± 1.1 °C) pre-treatments. No significant differences were found among groups. The overall (black, $n = 105$) average value (±S.E.) of CT_{min} was -6.5 ± 1.4 °C. (For interpretation of the references to colour in this figure legend, the reader is referred to the Web version of this article.)

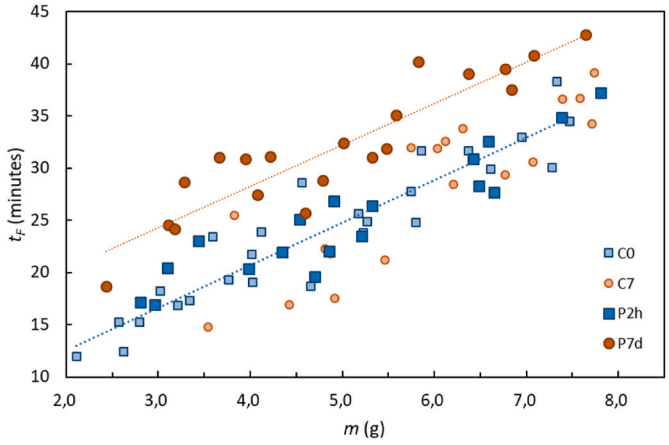

Fig. 6. Freezing time as a function of mass for C0 (light blue squares, $n = 26$), P2h (dark blue squares, $n = 18$), C7 (light brown circles, $n = 18$), and P7d (dark brown circles, $n = 20$) pretreatments. The lineal trends of basal C0 (blue dotted line) and P7d (brown dotted line) larvae are also shown. (For interpretation of the references to colour in this figure legend, the reader is referred to the Web version of this article.)

Table 3
Freezing time: ANCOVA and post-hoc pairwise comparisons.

ANCOVA			Post-hoc Tukey tests		
Factor	*F*	*P*	Pair comparison	*F*	*P*
Date	3.732	0.057	P7d vs C7	6.621	**< 0.001**
Mass	419.370	**< 0.001**	P7d vs C0	9.634	**< 0.001**
Pre-treatment	38.488	**< 0.001**	P7d vs P2h	6.886	**< 0.001**
			P2h vs C0	2.048	0.180
			P2h vs C7	0.258	0.994
			C0 vs C7	2.329	0.101

mass ($F = 8.204$, $P = 0.005$), as well as on the pretreatment group ($F = 3.318$, $P = 0.023$), while collection date had no significant effect ($F = 0.290$, $P = 0.592$). For control C0 larvae within different mass ranges ($m < 5$ g and $m \geq 5$ g), variations in their survival rates with temperature were then fitted to logistic regression models. Fig. 7a shows the basal (C0 larvae) survival rate at day 14 as a function of the exposure time after SCP detection. We found a high survival for exposures implying an almost complete freezing: 87% survival after 30 min of SCP detection. For longer exposures implying complete freezing and sub-freezing, survival was still 33% after 1 h of SCP detection and dropped to 0% for exposures longer than 2 h.

For an exposure time of 1 h after SCP detection, we also tested whether larvae with different pretreatments presented any significant difference in their freezing survival. We found (Fig. 7 and Table 4) that the survival rate of P7d-animals was significantly higher than for both C7- and C0-controls. No significant difference was found between the freezing survival of C0 and C7 groups. The P2h group had instead an intermediate freezing survival of 50%, not significantly different from that obtained for C0, C7, and P7d groups. We also observed (Fig. 7b) that, in C0, C7, and P2h larvae, the majority of deaths occurred during the freezing exposure itself (day 0). In contrast, the P7d group exhibited a different mortality trend, with deaths primarily occurring some days after the freezing exposure.

Note that, according to the previous Fig. 6, an exposure time of 1 h after the detection of SCP implies complete freezing even for the most massive larvae of the different pretreatment groups. This means that, in their individual freezing curves (see Fig. 1), all larvae ended in the sub-freezing stage with body temperatures (T_{end}) that, in most cases, had already decreased below SCP. On average, larvae from the P7d group ended with body temperatures close to SCP ($\Delta T = T_{end} - \text{SCP} = -0.2 \pm 0.4$ °C), while the C0- and C7-control groups ended with significantly ($P < 0.05$) lower temperatures, a few degrees below SCP: $\Delta T = -2.3 \pm 0.4$ °C (for C0) and $\Delta T = -1.8 \pm 0.4$ °C (for C7). These differences in final body temperature most likely come from the longer freezing times required by larvae after the P7d pretreatment. The P2h group had instead intermediate values ($\Delta T = -1.4 \pm 0.4$ °C), not statistically different from those obtained in the other groups.

3.4. Cold-induced morphological changes

Fig. 8 shows X-ray CT images that are representative of the inner morphology found for *Paysandisia archon* after different pretreatments. Each panel compares (from transverse, coronal, and sagittal views) larvae exposed to either short (C0 and P2h) or long (C7 and P7d) pre-treatments. This figure also shows that animals exposed to 1 °C for 7 days (P7d group) exhibited a qualitatively distinct internal morphology compared to the other larval groups. Indeed, animals in the P7d group had a comparatively thick integumentary system dominated by high-density tissues, while the fat body layer appeared less extensive than in the remaining groups.

Table 5 summarizes the quantitative results found for the morphological components in larvae from different pretreatment groups. We found that, except for the inner air, the volume of all components significantly varied among the different pretreatments ($P < 0.05$), while other factors such as the collection date ($P = 0.946$) or the larval mass ($P = 0.596$) did not have any significant effect. Compared to the other groups, P7d-larvae exhibited a significant reduction in all low-density components, particularly in hemolymph content, as well as a significant increase in the percentage of high-density tissues and digestive tract. In the P2h group, although the average components followed a similar trend, none of them showed a statistically significant change compared to the control values.

4. Discussion and conclusions

In this work, we analyzed for the first time the cold tolerance of *Paysandisia archon*. To this end, we measured the different thermal parameters: chill-coma onset temperature, median lethal temperature, supercooling point, freezing time and freezing survival. We also studied the possible effect on these parameters of several factors, such as the larval mass or the ability of cold hardening after a short or long pre-exposure to sub-lethal low temperatures.

A remarkable result found in the present study is the ability of

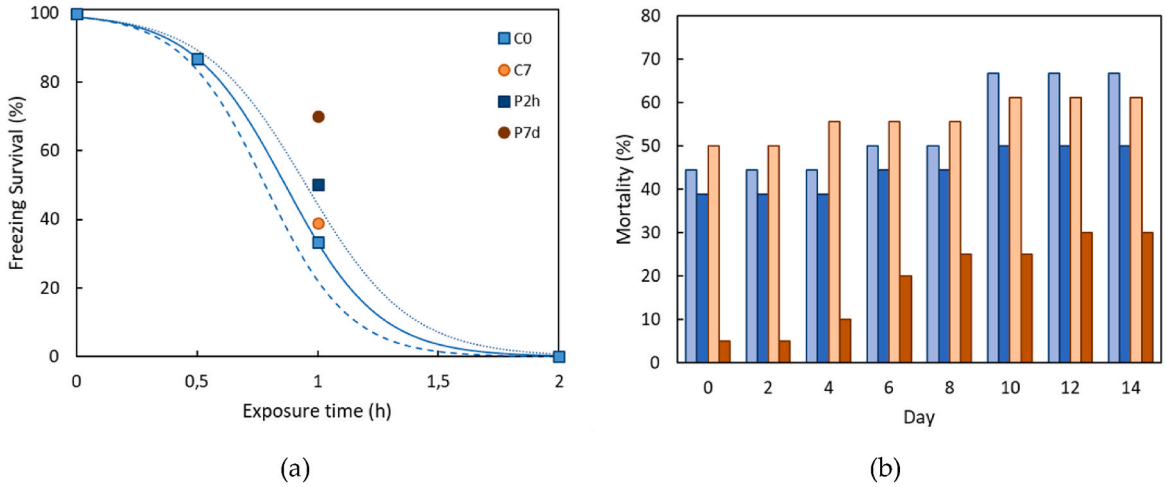

Fig. 7. a) Freezing survival at day 14 as a function of exposure time for C0 larvae (light blue squares, $n = 18$). Data were fitted to logistic regression models for all C0 larvae (solid curve), larvae with mass <5 g (dashed curve), and larvae with mass ≥5 g (dotted curve). For 1 h-freezing exposure, the figure also shows the survival rate for C7 (light brown circle, $n = 18$), P2h (dark blue square, $n = 18$), and P7d (dark brown circle, $n = 20$) groups, b) Cumulative mortality for 14 days after a 1 h-freezing exposure for C0 (light blue), C7 (light brown), P2h (dark blue), and P7d (dark brown) groups. (For interpretation of the references to colour in this figure legend, the reader is referred to the Web version of this article.)

Table 4
Survival rates after 1 h-freezing exposure and Post-hoc pairwise comparisons (Kaplan Meier analysis).

Grouping					*P* values			
Group	Survival	*L*	*W*	*T*	Pair	P_L	P_W	P_T
C0	33%	(a)	(a)	(a)	P7d vs C7	**0.030**	**0.011**	**0.017**
P2h	50%	(a, b)	(a, b)	(a, b)	P7d vs C0	**0.018**	**0.010**	**0.013**
C7	39%	(a)	(a)	(a)	P7d vs P2h	0.163	0.090	0.120
P7d	70%	(b)	(b)	(b)	P2h vs C0	0.375	0.484	0.428
					P2h vs C7	0.491	0.475	0.478
					C0 vs C7	0.874	0.932	0.982

Note: Different letters (*a,b*) denote groups with significant difference according to L = log-rank, W=Wilcoxon and T = Tarone-Ware tests.

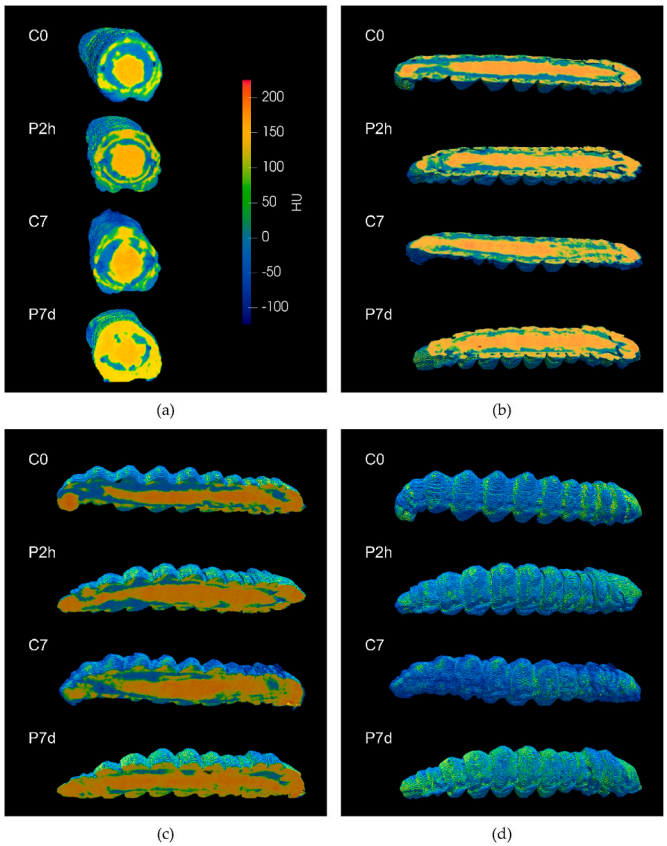

Fig. 8. Three-dimensional representation of the inner structure of *Paysandisia Archon* obtained from the X-ray CT system. Each panel compares larvae with short (C0 and P2h) and long (C7 and P7d) pre-treatments from a) transverse, b) coronal, c) sagittal, and d) exterior views.

Paysandisia archon to survive short periods of freezing. Generally, tropical insects are freeze-intolerant (LT_{50} > SCP) and, therefore, they die before ice forms within their body fluids. This has led some authors (e.g., Renault 2002) to question the ecological value of SCP for tropical species, as they rarely survive more than a few hours at temperatures close to 0 °C, while many of them have SCP as low as −12 °C. According to such authors, the supercooling ability of many of these insects could instead result from other adaptations unrelated to cold, such as resistance to desiccation. The SCP value (about −6.5 °C) found in the present study for *Paysandisia archon* is similar or even higher than those previously reported for other tropical or subtropical lepidopterans (e.g., Kim et al., 2017). However, we found that this species tolerated quite well (very low mortality) partial freezing, and was even able to survive (about 50% mortality) complete freezing (1 h after SCP detection). Indeed, we found that the median lethal temperature for this species was similar to its SCP. This is a rather surprising result, since all other lepidopterans native to warm areas are clearly freeze-intolerant, with LT_{50} values much higher (up to 12 °C higher, Terblanche et al., 2017) than SCP. In tropical insects, the ability to survive partial freezing was previously reported for the cockroach *Gromphadorhina coquereliana* (Lubawy et al., 2019). Nevertheless, our results represent the first study reporting a moderately freeze-tolerant tropical lepidopteran. We then conclude that the SCP and LT_{50} values for *Paysandisia archon* do not constitute a very severe barrier to the expansion of this species towards temperate zones.

The key thermal factor limiting the expansion of this species appears to be the value found for CT_{min} (6.5 °C), implying that *Paysandisia archon*

Table 5
Inner components: average values (±S.E.) for the different pre-treatment groups.

Group	Inner air	Hemolymph	Fat body	HD tissues	Digestive tract
C0	$3 \pm 1\%^{(a)}$	$14 \pm 2\%^{(b)}$	$39 \pm 5\%^{(d)}$	$24 \pm 7\%^{(h)}$	$20 \pm 3\%^{(f)}$
P2h	$4 \pm 1\%^{(a)}$	$12 \pm 1\%^{(b)}$	$33 \pm 4\%^{(d)}$	$30 \pm 7\%^{(h)}$	$20 \pm 3\%^{(f)}$
C7	$3 \pm 1\%^{(a)}$	$13 \pm 3\%^{(b)}$	$33 \pm 5\%^{(d)}$	$31 \pm 6\%^{(h)}$	$20 \pm 3\%^{(f)}$
P7d	$3 \pm 2\%^{(a)}$	$6 \pm 3\%^{(c)}$	$24 \pm 7\%^{(e)}$	$43 \pm 9\%^{(i)}$	$24 \pm 3\%^{(g)}$

Note: Identical superscripts denote averages without significant differences (Tukey tests with $P > 0.05$).

cannot remain fully active in regions with moderately cold winters. In other tropical or subtropical lepidopterans, CT_{min} is usually above 8 °C (Klok and Chown, 1998; Uyi et al., 2017; Stotter and Terblanche 2009; Au and Bonebrake, 2019) and constitutes an important barrier to their expansion, since prolonged inactivity can compromise reaching a sufficient number of generations per year to maintain a stable population. The same is observed for other orders of insects native to warm regions (e.g., Coulin et al., 2019). These drawbacks are partially mitigated in *Paysandisia archon*, which overwinters thermally protected inside the palm tree, where it continues its development through different larval stages (Sarto i Monteys and Aguilar, 2005; Muñoz-Adalia and Colinas 2020).

Another relevant aspect addressed in the present study was the response of this species to a short or long pre-exposure to moderately low temperatures. In particular, we analyzed potential cold-induced morphological changes and their possible correlation with an improvement in the subsequent tolerance to more severe cold conditions. As in a previous work (León-Quinto et al., 2024), we found that prolonged exposure to moderately low temperatures (1 °C for 7 days) produces a hardening and thickening of the integument of this species, as well as a significant decrease in hemolymph content. Such changes occurred gradually, and they were not still significant after a short exposure (for 2 h) to the same temperature. Our study did not allow us to determine the processes that led to this cold-induced reduction in water content. Nevertheless, the observed increase in the volume of the digestive tract suggests that part of the water loss could result from a progressive transfer of water from the hemolymph to the digestive tract, from where a certain amount might have been expelled to the outside. This transfer probably had its origin in a temporary and reversible imbalance of osmoregulation caused by cold stress, similar to that found by MacMillan et al. (2012) for insects in chill-coma. In any case, whatever its origin, a decrease in water volume increases the chances that a larva can survive a short freezing event. Indeed, a reduction in water content has been previously reported for some overwintering Coleoptera (Lundheim and Zachariassen, 1993) and Lepidoptera (Kojic et al., 2010; Shao et al., 2018) as a cryoprotective strategy to reduce damage from freezing of biofluids and to increase the concentration of cryoprotective substances.

Our results also suggest an additional cryoprotective function of partial dehydration. Indeed, a reduction in water content implies a decrease in the thermal conductivity (k) of the larvae, since water is a much more efficient thermal conductor ($k_{water} = 2.2$ W m^{-1} K^{-1}, $k_{ice} = 0.54$ W m^{-1} K^{-1}) than other relevant components ($k_{fat} = k_{protein} = 0.18$ W m^{-1} K^{-1}) (e.g., Becker and Fricke 2003). Therefore, animals with reduced water content slow down the release of latent heat from their inner freezing front to the outside, which may partially account for their significantly longer freezing times, thus improving their ability to survive short periods of freezing. In addition, the biochemical response to cold, part of which was recently studied (León-Quinto et al., 2024), may also have played a relevant role in the thermal properties of this species.

The observed increase in freezing survival for this species after prolonged cold pre-exposure was accompanied by only a very modest (if any) improvement in other parameters that characterize its cold tolerance. Actually, the SCP and CTmin values found for the control animals did not exhibit significant changes when the larvae were subjected to either a short or long pre-exposure to moderately low temperatures. Therefore, we found no correlation between SCP and the water content of pre-treated larvae. Such independence of SCP and water content was previously observed in some other species (e.g. Zheng et al., 2018; Vrba et al., 2022), while many others evidenced a clear correlation (e.g. Block 2002). The relationship between SCP and water content is very complex and each case requires specific study. It depends on multiple factors, some with opposing effects on SCP, including the level of antifreeze compounds or the presence and activity of different ice-nucleating agents (proteins, bacteria …).

Concerning the median lethal temperature, LT_{50}, animals exposed to short cold pretreatment did not exhibit any significant change compared to controls. Their survival rate at −8 °C was nearly the same (about 40–50%) as for control animals. Therefore, we concluded that this species did not show a capacity for rapid cold hardening. On the opposite, the survival rate at −8 °C increased to 75% for larvae having long prior contact with a sublethal low-temperature environment. Such an improvement was significant according to different statistical tests (Wilcoxon and Tarone-Ware tests), but still compatible with the experimental uncertainty for the log-rank test. Our results then suggest that *Paysandisia archon* has a certain capacity to improve its tolerance to severe cold events when they have been preceded by a sufficiently long period of moderately low temperatures. This improvement could be associated, at least in part, with increased resistance to brief episodes of freezing.

Summarizing, the results found in the present study indicate that *Paysandisia archon* has a cold tolerance much greater than expected for a tropical insect. It can survive occasional events of severe cold, even short periods of complete freezing, especially if such events have been preceded by a few transition days with moderately cold temperatures. As a matter of fact, in the last decade, this species has begun to be detected in temperate regions of northern Europe. Currently, these are only isolated detections, but the sporadic presence of *Paysandisia archon* in these regions has been interpreted as evidence of its tendency to expand its range toward northern areas (Couturier 2017).

Funding

Financial support was provided by the project PAR UMH (Universidad Miguel Hernandez, Spain).

CRediT authorship contribution statement

Trinidad León-Quinto: Writing – original draft, Visualization, Supervision, Methodology, Investigation, Funding acquisition, Data curation, Conceptualization. **Noelia Antón-Ruiz:** Investigation, Data curation. **Roque Madrigal:** Visualization, Investigation, Data curation. **Arturo Serna:** Writing – original draft, Visualization, Supervision, Methodology, Investigation, Funding acquisition, Formal analysis, Data curation, Conceptualization.

Declaration of competing interest

The authors declare that they have no known competing financial interests or personal relationships that could have appeared to influence the work reported in this paper.

Acknowledgments

Special thanks to Victoria Martínez, Natalia Penalva, Paula Toledo and José Juan López Calatayud from the public company TRAGSA for providing us with the *Paysandisia archon* larvae. We are indebted to them for their great support and enthusiasm in helping us.

References

Andersen, M.K., Jensen, S.O., Overgaard, J., 2017. Physiological correlates of chill susceptibility in Lepidoptera. J. Insect Physiol. 98, 317–326. https://doi.org/10.1016/j.jinsphys.2017.02.002.

ASHRAE, 2006. Cooling and freezing times of food. In: 2006 ASHRAE Handbook: Refrigeration). ISBN- 9781601197948.

Au, T.F., Bonebrake, T.C., 2019. Increased suitability of poleward climate for a tropical butterfly (euripus nyctelius) (Lepidoptera: nymphalidae) accompanies its successful range expansion. J. Insect Sci. 19, 2. https://doi.org/10.1093/jisesa/iez105.

Bathiany, S., Dakos, V., Scheffer, M., Lenton, T.M., 2018. Climate models predict increasing temperature variability in poor countries. Sci. Adv. 4, 1–10. https://doi.org/10.1126/sciadv.aar580.

Becker, B.R., Fricke, B.A., 2003. Freezing. Principles. In: Encyclopedia of Food Sciences and Nutrition. Academic Press, pp. 2706–2711. https://doi.org/10.1016/B0-12-227055-X/00521-6. ISBN 9780122270550.

Block, W., 2002. Interactions of water, ice nucleators and desiccation in invertebrate cold survival. Eur. J. Entomol. 99, 259–266. https://doi.org/10.14411/eje.2002.035.

Caesar, A.J., 2003. Synergistic interaction of soilborne plant pathogens and root-attacking insects in classical biological control of an exotic rangeland weed. Biol. Control 28, 144–153. https://doi.org/10.1016/S1049-9644(03)00053-7.

Chowanski, S., Lubawy, J., Paluch-Lubawa, E., Spochacz, M., Rosiński, G., Słocińska, M., 2017. The physiological role of fat body and muscle tissues in response to cold stress in the tropical cockroach Gromphadorhina coquereliana. PLoS One 12, e0173100. https://doi.org/10.1371/journal.pone.0173100.

Chowanski, S., Lubawy, J., Spochacz, M., Ewelina, P., Grzegorz, S., Rosinski, G., Slocinska, M., 2015. Cold induced changes in lipid, protein and carbohydrate levels in the tropical insect Gromphadorhina coquereliana. Comp. Biochem. Physiol. Mol. Integr. Physiol. 183, 57–63. https://doi.org/10.1016/j.cbpa.2015.01.007.

Coulin, C., de la Vega, G.J., Chifflet, L., Calcaterra, L.A., Schilman, P.E., 2019. Linking thermo-tolerances of the highly invasive ant, Wasmannia auropunctata, to its current and potential distribution. Biol. Invasions 21, 3491–3504. https://doi.org/10.1007/s10530-019-02063-0.

Couturier, G., 2017. Présence de Paysandisia archon Burmeister, 1880, dans la région parisienne (Lepidoptera, Castniidae). Bull. Société Entomologique de France 122, 72–74. https://doi.org/10.3406/bsef.2017.3177.

Cubillos, C., Cáceres, J.C., Villablanca, C., Villarreal, P., Baeza, M., Cabrera, R., Graether, P., Veloso, C., 2018. Cold tolerance mechanisms of two arthropods from the andean range of Central Chile: agathemera crassa (insecta: agathemeridae) and euathlus condorito (arachnida: theraphosidae). J. Therm. Biol. 74, 133–139. https://doi.org/10.1016/j.jtherbio.2018.03.018.

de la Vega, G.J., Medone, P., Ceccarelli, S., Rabinovich, J., Schilman, P.E., 2015. Geographical distribution, climatic variability and thermo-tolerance of Chagas disease vectors. Ecography 38, 851–860. https://doi.org/10.1111/ecog.01028.

Denlinger, D.L., Lee, R.E., 2010. Low Temperature Biology of Insects. Cambridge University Press, Cambridge, United Kingdom. https://doi.org/10.1017/CBO9780511675997.

Huey, R.B., Crill, W.D., Kingsolver, J.G., Weber, K.E., 1992. A method for rapid measurement of heat or cold resistance of small insects. Funct. Ecol. 6, 489–494.

Johnson, N.C., Xie, S.P., Kosaka, Y., et al., 2018. Increasing occurrence of cold and warm extremes during the recent global warming slowdown. Nat. Commun. 9, 1724. https://doi.org/10.1038/s41467-018-04040-y].

Kang, T., You, Y., Jun, S., 2020. Supercooling preservation technology in food and biological samples: a review focused on electric and magnetic field applications. Food Sci. Biotechnol. 29, 303–321. https://doi.org/10.1007/s10068-020-00750-6.

Kim, Y., Lee, D.W., Jung, J.K., 2017. Rapid cold-hardening of a subtropical species, maruca vitrata (Lepidoptera: crambidae), accompanies hypertrehalosemia by upregulating trehalose-6-phosphate synthase. Environ. Entomol. 46, 1432–1438. https://doi.org/10.1093/ee/nvx153.

Kleynhans, E., Mitchell, K.A., Conlong, D.E., Terblanche, J.S., 2014. Evolved variation in cold tolerance among populations of Eldana saccharina (Lepidoptera: Pyralidae) in South Africa. J. Evol. Biol. 27, 1149–1159. https://doi.org/10.1111/jeb.12390.

Klok, C.J., Chown, S.L., 1998. Field thermal ecology and water relations of gregaria phase African armyworm caterpillars, Spodoptera exempta (Lepidoptera: noctuidae). J. Therm. Biol. 23, 131–142. https://doi.org/10.1016/S0306-4565(97)00068-5.

Kojic, D., Purac, J., Popovic, Z.D., Pamer, E., Grubor-Lajsic, G., 2010. Importance of the body water management for winter cold survival of the European corn borer ostrinia nubilalis hübn. (Lepidoptera: Pyralidae). Biotechnol. Biotechnol. Equip. 24, 648–654. https://doi.org/10.1080/13102818.2010.10817915.

Koštál, V., Korbelová, J., Štětina, T., Poupardin, R., Colinet, H., Zahradníčková, H., Opekarová, I., Moos, M., Šimek, P., 2016. Physiological basis for low temperature survival and storage of quiescent larvae of the fruit fly Drosophila melanogaster. Sci. Rep. 6, 1–11. https://doi.org/10.1038/srep32346, 32346.

Lencioni, V., 2004. Survival strategies of freshwater insects in cold environments. J. Limnol. 63, 45–55. https://doi.org/10.4081/jlimnol.2004.s1.45.

León-Quinto, T., Fimia, A., Madrigal, R., Serna, A., 2020. Morphological response of the red palm weevil, *Rhynchophorus ferrugineus*, to a transient low temperature analyzed by computer tomography and holographic microscopy. J. Therm. Biol. 94, 102748 https://doi.org/10.1016/j.jtherbio.2020.102748.

León-Quinto, T., Serna, A., 2022. Cryoprotective response as part of the adaptive strategy of the red palm weevil, Rhynchophorus ferrugineus, against low temperatures. Insects 13, 134. https://doi.org/10.3390/insects13020134.

León-Quinto, T., Madrigal, R., Cabello, E., Fimia, A., Serna, A., 2024. Morphological and biochemical responses of a Neotropical pest insect to low temperatures. J. Therm. Biol. 119, 103795 https://doi.org/10.1016/j.jtherbio.2024.103795.

Lubawy, J., Daburon, V., Chowanski, S., Słocińska, M., Colinet, H., 2019. Thermal stress causes DNA damage and mortality in a tropical insect. J. Exp. Biol. 222, jeb213744 https://doi.org/10.1242/jeb.213744.

Lundheim, R., Zachariassen, K.E., 1993. Water balance of over-wintering beetles in relation to strategies for cold tolerance. J. Comp. Physiol. B 163, 1–4. https://doi.org/10.1007/BF00309658.

MacMillan, H.A., Williams, C.M., Staples, J.F., Sinclair, B.J., 2012. Reestablishment of ion homeostasis during chill-coma recovery in the cricket Gryllus pennsylvanicus. Proc. Natl. Acad. Sci. USA 109, 20750–20755. https://doi.org/10.1073/pnas.1212788109.

Martin, M.M., Cabello, T., 2005. Biología y ecología del curculiónido rojo de la palmera, Rhynchophorus ferrugineus. Universidad de Almería, Spain, pp. 1–202. ISBN 84-689-5292-3.

Martin, M.M., Cabello, T., 2006. Manejo de la cría del picudo rojo de la palmera, Rhynchophorus ferrugineus (Olivier, 1790) (Coleoptera, Dryophthoridae), en dieta artificial y efectos en su biometría y biología. Bol. Sanid. Vegetal Plagas 32, 631–641.

Muñoz-Adalia, E.J., Colinas, C., 2020. The invasive moth Paysandisia archon in Europe: biology and control options. J. Appl. Entomol. 144, 341–350. https://doi.org/10.1111/jen.12746.

Mutamiswa, R., Chidawanyika, F., Nyamukondiwa, C., 2018a. Comparative assessment of the thermal tolerance of spotted stemborer, Chilo partellus (Lepidoptera: crambidae) and its larval parasitoid, Cotesia sesamiae (Hymenoptera: braconidae). Insect Sci. 25, 847–860. https://doi.org/10.1111/1744-7917.12466.

Mutamiswa, R., Chidawanyika, F., Nyamukondiwa, C., 2018b. Superior basal and plastic thermal responses to environmental heterogeneity in invasive exotic stemborer Chilo partellus Swinhoe over indigenous Busseola fusca (Fuller) and Sesamia calamistis Hampson. Physiol. Entomol. 43, 108–119. https://doi.org/10.1111/phen.12235.

Mutamiswa, R., Mbande, A., Nyamukondiwa, C., Chidawanyika, F., 2023. Thermal adaptation in Lepidoptera under shifting environments: mechanisms, patterns, and consequences. Phytoparasitica 51, 929–955. https://doi.org/10.1007/s12600-023-01095-6.

Pham, Q.T., 2014. Food Freezing and Thawing Calculations. Springer. https://doi.org/10.1007/978-1-4939-0557-7.

Renault, D., 2002. Survival at low temperatures in insects: what is the ecological significance of the supercooling point? Cryoletters 23, 217–228.

Roeder, K.A., Daniels, J.D., 2022. Thermal tolerance of western corn rootworm: critical thermal limits, knock-down resistance, and chill coma recovery. J. Therm. Biol. 109, 103338 https://doi.org/10.1016/j.jtherbio.2022.103338.

Rozsypal, J., Košťál, V., 2018. Supercooling and freezing as eco-physiological alternatives rather than mutually exclusive strategies: a case study in Pyrrhocoris apterus. J. Insect Physiol. 111, 53–62. https://doi.org/10.1016/j.jinsphys.2018.10.006.

Sánchez, F., Orero, A., Soriano, A., Correcher, C., Conde, P., González, A., Hernández, L., Moliner, L., Rodríguez-Alvarez, M.J., Vidal, L.F., Benlloch, J.M., Chapman, S.E., Leevy, W.M., 2013. ALBIRA: a small animal PET/SPECT/CT imaging system. Med. Phys. 40, 1–11. https://doi.org/10.1118/1.4800798.

Sarto i Monteys, V., Aguilar, L., 2005. The castniid palm borer, Paysandisia archon (burmeister, 1880), in Europe: comparative biology, pest status and possible control methods (Lepidoptera: castniidae). Nachr. entomol. Ver. Apollo 26, 61–94. https://doi.org/10.13140/2.1.4565.6966.

Shao, Y.Y., Feng, Y.Q., Tian, B., Wang, T., He, Y.H., Zong, S.X., 2018. Cold hardiness of larvae of *Dendrolimus tabulaeformis* (Lepidoptera: lasiocampidae) at different stages during the overwintering period. Eur. J. Entomol. 115, 198–207. https://doi.org/10.14411/eje.2018.018.

Sinclair, B.J., Coello Alvarado, L.E., Ferguson, L.V., 2015. An invitation to measure insect cold tolerance: methods, approaches, and workflow. J. Therm. Biol. 53, 180–197. https://doi.org/10.1016/j.jtherbio.2015.11.003.

Stotter, R.L., Terblanche, J.S., 2009. Low-temperature tolerance of false codling moth *Thaumatotibia leucotreta* (Meyrick) (Lepidoptera: tortricidae) in South Africa. J. Therm. Biol. 34, 320–325. https://doi.org/10.1016/j.jtherbio.2009.05.002.

Terblanche, J.S., Mitchell, K.A., Uys, W., Short, C., Boardman, L., 2017. Thermal limits to survival and activity in two life stages of false codling moth Thaumatotibia leucotreta (Lepidoptera, Tortricidae). Physiol. Entomol. 42, 379–388.

Toxopeus, J., Sinclair, B., 2018. Mechanisms underlying insect freeze tolerance. Biol. Rev. 93, 1891–1914. https://doi.org/10.1111/brv.12425.

Uyi, O., Zachariades, C., Marais, E., Hill, M., 2017. Reduced mobility but high survival: thermal tolerance and locomotor response of the specialist herbivore, Pareuchaetes insulata (Walker) (Lepidoptera: erebidae), to low temperatures. Bull. Entomol. Res. 107, 448–457. https://doi.org/10.1017/S0007485316001103.

Vrba, P., Sucháckova-Bartonová, A., Andres, M., Nedved, O., Šimek, P., 2022. Exploring cold hardiness within a butterfly clade: supercooling ability and polyol profiles in European satyrinae. Insects 13, 369. https://doi.org/10.3390/insects13040369.

Zheng, X.-L., Liu, J., Huang, X.-Y., Meng, L.-Y., Li, J., Lu, W., 2017. Cold hardiness of *Phauda flammans* (Lepidoptera: zygaenidae) larvae. Entomol. Fennica 28, 9–15. https://doi.org/10.33338/ef.84670.

Zheng, X.-L., Wang, P., Liu, J., Zhang, Y.-J., Li, J., Lu, W., 2018. Supercooling capacity of the sweet potato leaf folder, brachmia macroscopa meyrick (Lepidoptera: gelechiidae). Pakistan J. Zool. 50, 779–782. https://doi.org/10.17582/journal.pjz/2018.50.2.sc5.